

PAPER • OPEN ACCESS

Optimization of a ventilation system integrated into a window frame using CFD simulations

To cite this article: J. Karolin and M. Rahiminejad 2023 *J. Phys.: Conf. Ser.* **2600** 082016

View the [article online](#) for updates and enhancements.

You may also like

- [Heat Recovery Ventilation Systems and their Physical Quantification](#)
Boris Bielek, Daniel Szabó, Josip Klem et al.
- [Supply Ventilation and Prevention of Carbon Monoxide \(II\) Ingress into Building Premises](#)
N A Litvinova
- [Effect of mechanical ventilation on air infiltration rate in a concert hall](#)
Yuchen Shi and Xiaofeng Li

PRIME
PACIFIC RIM MEETING
ON ELECTROCHEMICAL
AND SOLID STATE SCIENCE

HONOLULU, HI
Oct 6–11, 2024

Abstract submission deadline:
April 12, 2024

Learn more and submit!

Joint Meeting of
The Electrochemical Society
•
The Electrochemical Society of Japan
•
Korea Electrochemical Society

Optimization of a ventilation system integrated into a window frame using CFD simulations

J. Karolin¹, M. Rahiminejad¹

¹ Bern University of Applied Sciences, Biel/Bienne, Switzerland

joel.karolin@bfh.ch, mohammad.rahiminejad@bfh.ch

Abstract. A decentralized ventilation system has the potential to decrease the pressure drop in a ventilation system and consequently, increase the efficiency of the system and building skin. Including a decentralized ventilation system in a window cavity allows independent regulation of the fresh air quality in each room and can be easily installed without any additional brickwork. In this study, a novel ventilation system integrated into a window-frame is examined and the most critical region regarding pressure drop is identified using computational fluid dynamic (CFD) simulations. The entire fresh air channel including the optimized section is compared with the original volume regarding system resistance and satisfaction of the required airflow according to Swiss standards. The results suggest a relocation of the restricting control unit and an increased cross-section to decrease the air velocity and the pressure drop. The simulations predicted that the required airflow for sufficient indoor air quality is exceeded using the optimized geometry.

1. Introduction

In centralized ventilation systems, the operational equipment is stored and accommodated in one location. Therefore, long ducts with a high-pressure drop in the ventilation system require strong fans to compensate for the system resistance [1]. This means that high energy demand is needed to provide adequate air exchange inside a building [2] [3] [4]. Compared to the centralized ventilation systems, the higher efficiency and the significantly compacter design of decentralized ventilation systems due to the less pressure loss through the short tubing, make them a proper choice for renovation and reconstruction projects in buildings. Among various solutions using the window cavity [5] [6], the use of window frames to house a decentralized ventilation system has been recently shown as a promising idea to provide fresh air into indoor space. The compact integration of a decentralized ventilation system in a space-limited window cavity offers a convenient installation and prevents additional brickwork.

Computational fluid dynamics (CFD) is a widely used method in research and industry to investigate the thermo-hydrodynamic performance of novel products. Nowadays, it is used in various fields for performance forecasting while it also saves development costs. Classical dimensioning of ventilation systems is generally performed with tables, charts, and hand calculations. CFD simulation, however, is a resealable method for compact and complex ventilation systems, where the impact of geometrical improvement on the behavior of the airflow could be reliably captured. This would certainly result in a better final product performance before the manufacturing process.

In the present study, indoor air ventilation through a novel window-frame structure, as shown in Figure 1, is numerically investigated. The analysis is performed using CFD simulations to address the optimized solution for the geometry of the window frame. In pursuance of better energy efficiency of the entire ventilation system, the airflow behavior and recirculation area at the most critical point are analyzed. Throughout this process, the airflow entering the indoor space is obtained assuming



different scenarios to fulfill the minimum value required by Swiss standards for mechanical ventilation in residential buildings [7].

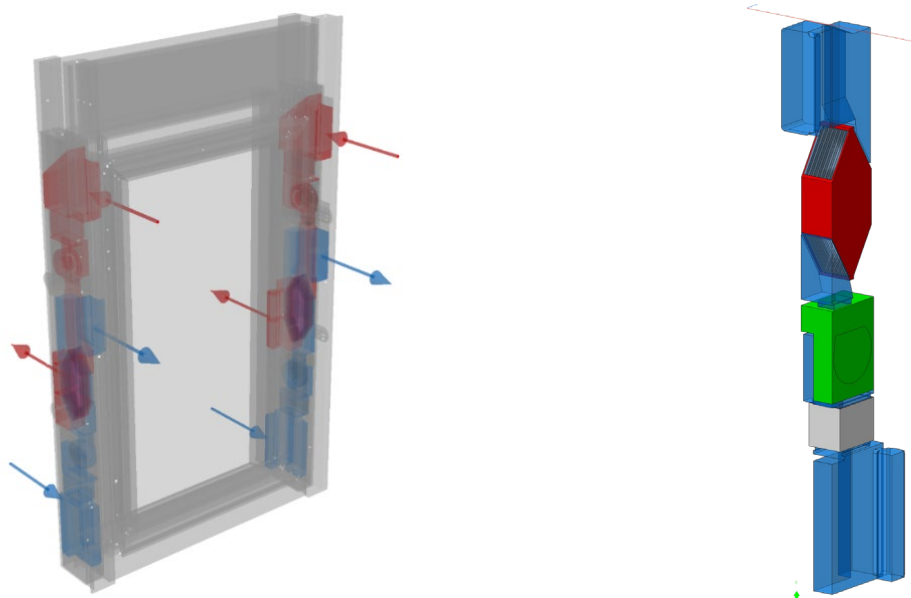


Figure 1. Schematic functionality of the ventilation system (fresh air and exhaust air channel) integrated in a window (left) and the schematic fresh air channel (right) including the components, namely filter, centrifugal fan, and heat exchanger.

2. Theory

2.1. Concept of the Assessed Window Frame

The novel window structure, shown in Figure 1, accommodates a decentralized ventilation system consisting of a window frame and glazing. The window frame is composed of two vertical elements which both contain an autonomous ventilation system consisting of a fresh air and an exhaust air channel both including a filter, centrifugal fan, and a heat exchanger. The air filter prevents dust, insects, and other particles from entering the system. The heat exchanger recovers heat between air streams from one to the other channel.

2.2. Requirements according to Swiss Standards

According to the Swiss Society of Engineers and Architects (SIA) standard number 382, part 5 [7] a fresh airflow of 30 m³ per hour and per room is recommended to be provided by mechanical ventilation systems in residential buildings. Based on the window concept described earlier, only half of the recommended airflow (15 m³/h) is required to be delivered by each fresh air channel.

2.3. Operational Point of a Ventilation System

Within a ventilation system, resistance occurs due to energy dissipation effects such as friction, turbulences, and separation between airflow and surface. The resistance of a system, obtained as a pressure drop from the inlet to the outlet of the system, is an exponential function of the airflow rate. It can be expressed as the system resistance curve of a ventilation channel.

A fan inside the ventilation system is supposed to deliver a certain pressure jump in order to compensate for the system resistance and therefore, push airflow through the system. Each fan is characterized by a fan specification curve at a specific speed, expressed as a function of pressure jump and airflow rate.

The intersection point of the resistance curve and the fan specification curve indicates the theoretical point of operation (pressure drop/jump [Pa] at a given airflow rate [m³/h]). The operational point of the ventilation system investigated in this study is further discussed in section 4.3.

3. Methodology

3.1. Mesh Generation

The model in this study, depending on the geometry, shows a partly structured mesh. Where a structured grid was not able to be applied, an unstructured tetrahedral grid is used. The grid of the examined ventilation channel consists of 9'147'606 cells. The grid size of 1 mm is obtained from the grid study analysis in section 4.1. To properly capture the boundary layer phenomenon close to the walls, a maximum of 5 layers for the inflation layer are added. The maximum growth rate is limited to 1.2 between inflation layers and the transition ratio is set to 0.272.

3.2. Solver Settings

For this study, the standard air properties, given by Ansys FLUENT, are used. The incompressible flow condition is assumed for the air moving in the system due to its relatively low speed. This means that the change in density is less than 5 % and can be neglected for this study.

In compliance with the aim of the study, i.e., the improvement of the airflow and optimization of the incorporated geometries, no heat transfer modes, namely conduction, convection, and radiation are considered.

The steady-state simulations are solved using the two-equation $k-\omega$ with the shear stress transport (SST) model [8] to capture the near-wall region and switch to the $k-\epsilon$ method in the free shear flow. The pressure-velocity coupling is done with the RANS algorithm.

3.3. Boundary Conditions

The inlet boundary condition at the opening of the fresh air is applied as the inlet velocity based on the design points for the system resistance curve. A zero-gauge pressure is considered in the outlet opening adjacent to the indoor space. The specification curves of the filter and fan elements provided by the manufacturers are used to apply the boundary condition in the interfaces of the components.

4. Results

4.1. Grid Sensitivity Analysis

The grid sensitivity analysis is performed using 3 models with different grid sizes for one section of the ventilation channel located after the centrifugal fan and before the heat exchanger. This area is selected due to the occurrence of higher airspeed and turbulences in the airflow after the fan outlet.

The pressure and velocity profiles obtained along a polyline in the examined section are depicted in Figure 2. The results show a similar trend for all three grid sizes. While the lines for grid sizes of 1 mm and 0.5 mm show a maximum difference of 2.4 % for the pressure and 0.7 % for the velocity, the difference between the 1 mm and 2 mm grid sizes reaches up to 5.7 % for pressure and 2.4 % for velocity.

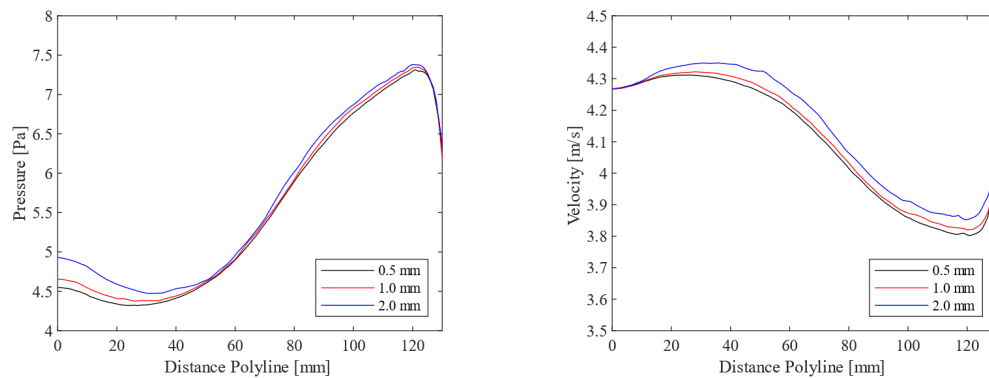


Figure 2. Grid Sensitivity Analysis for gauge pressure (left) and velocity (right). Comparison between 2 mm, 1 mm, and 0.5 mm grid sizes for a turbulent area within the system.

Based on this grid study, it can be concluded that a 1 mm grid leads to more accurate results compared to a 2 mm grid, but at a lower computational cost compared to the finer 0.5 mm grid. Therefore, the CFD simulations are conducted with this mesh size.

4.2. Optimization

The optimization of the geometry is conducted where the highest pressure drop in the system occurs and consequently, the acceleration of the air inside the system happens. This area is located where the control unit of the ventilation system was originally intended to be placed. This part of the fresh air channel starts after the inlet section and ends at the location of the filter. The geometries shown in Figure 3 and Figure 4 represent the optimization considered in the model. The left side of both figures shows the volume limited by the control unit while the right side shows the volume with a relocated control unit.

The streamlines indicating the relative pressure within the section under consideration before (left) and after (right) the optimization are presented in Figure 3. The weighted average of the static pressure shows a pressure drop from the inlet to the outlet of 112.1 Pa before and 3.2 Pa after the optimization.

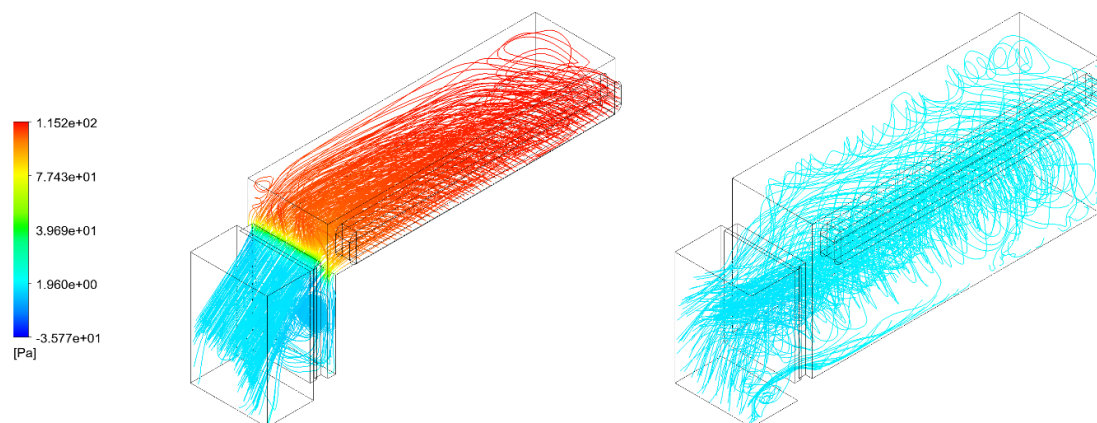


Figure 3. Streamline showing the pressure drop before (left) and after (right) the optimization.

The velocity streamlines in the examined section are shown in Figure 4. The weighted average inlet velocity is 1.41 m/s for both optimization stages. For the outlet, the weighted average velocity before the optimization obtains 2.79 m/s compared to 1.50 m/s for the optimized geometry.

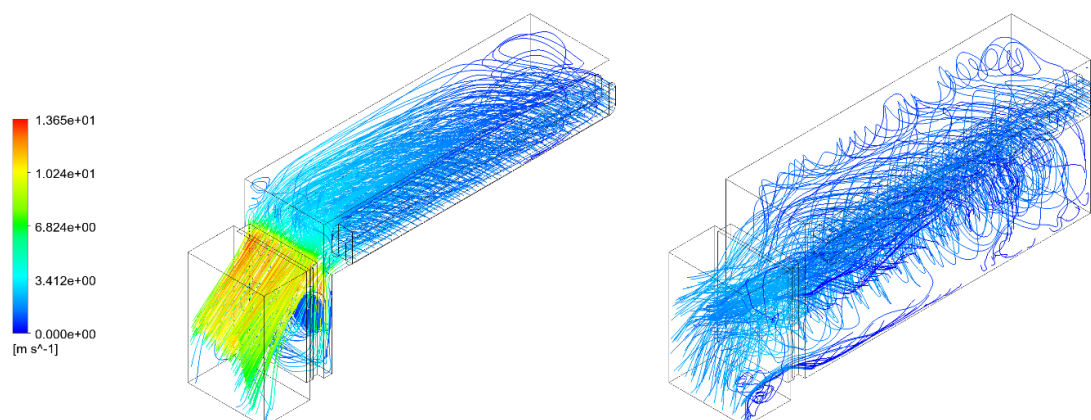


Figure 4. Streamline showing the velocity before (left) and after (right) the optimization.

The results in Figure 3 and Figure 4 reveal that the optimized geometry has resulted in a more efficient flow movement through the system, which reduces the pressure drop and increases the airflow provided to the indoor space.

4.3. Point of Operation

The system resistance curves before and after the optimization, the fan specification curve, and the resulting two points of operation are plotted in Figure 5. The predicted airflow in the initial system geometry results in $13.4 \text{ m}^3/\text{h}$ at 166.2 Pa , while the optimized geometry shows an increment of 52.2% in airflow rate reaching $20.4 \text{ m}^3/\text{h}$ at 120.5 Pa .

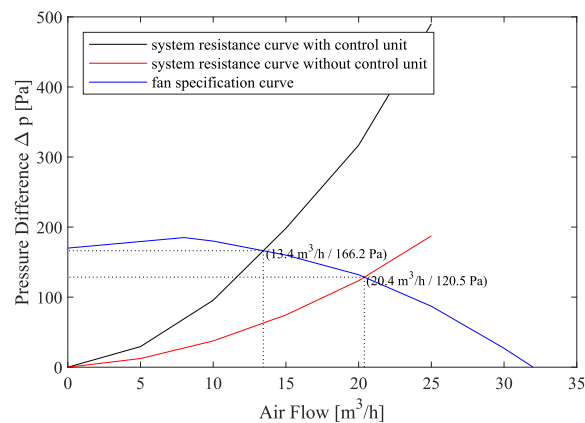


Figure 5. Points of operation given where the system resistance curves of the original system with the control unit (-) and the improved geometry without the control unit (-) intersect the fan specification curve (-).

5. Discussion

The results in the previous section show a decrement in the pressure loss in the ventilation system of 108.9 Pa at a flow rate of $15 \text{ m}^3/\text{h}$ and a drop in weighted average speed at the outlet of the considered section of 1.29 m/s . This significant difference in the adapted geometry can be explained by the absence of the relatively small opening within the section that led to an acceleration of the airstream and consequently, a significant pressure drop in the system.

These improvements additionally impact the efficiency of the filter. The filter specification curve is a function of airflow and pressure drop. The latter exponentially increases with increasing airflow. Therefore, a lower weighted average velocity over increased cross-section results in a reduced pressure drop due to the filter.

The resulting streamlines in the original geometry show the separating of the air stream at the point of the critical cross-section, which leads to a smaller passed-through area at the location of the filter and therefore, results in a notable increase in the weighted average airspeed. These effects are eliminated by relocating the control unit and extending the cavity. Consequently, the velocity gradient over the outlet cross-section could be decreased.

These improvements in geometry impact the operational points and increase the airflow by $7.0 \text{ m}^3/\text{h}$ to a value of $20.4 \text{ m}^3/\text{h}$ while the pressure drop at the operational points is decreased by 45.7 Pa .

6. Conclusions

The impact of geometry optimization on the performance of the airflow in a ventilation system integrated into a window frame was investigated in this study. Due to the complexity of the problem, the CFD simulations were employed to numerically analyze the pressure and velocity distribution through the system before and after optimization.

Due to these reductions in pressure drop and improved airflow behavior in the fresh air channel, the maximum airflow exceeds the requirement according to SIA 382 – 5 [7]. It should be mentioned that this is a theoretical operational point of the system, and some reductions are expected in actual conditions due to the manufacturing process and other effects not captured in the simulation. Nevertheless, the computational results are promising regarding fresh air supply.

Achieving an airflow higher than the minimum requirement by the standards allows for reducing the speed of the fan, which leads to the reduced energy consumption of the system. At the same time, the noise emission can be reduced which is in favor of the occupant's comfort.

In the next steps, further geometrical optimizations will be examined so that recirculation zones in the entire ventilation system can be captured and possibly eliminated. Furthermore, the thermal analysis will be conducted to quantify the heat recovery between the fresh air and the exhaust air. The use of an efficient heat recovery system as well as a room-independent ventilation system could strongly contribute to the energy strategies by 2050 to effectively reduce carbon footprint emissions in society.

7. Acknowledgment

This work was supported by the Bern University of Applied Sciences (BFH) and Wenger Fenster AG under the framework of an InnoSuisse Project. We gratefully thank Prof. Bernhard Letsch for integrating this study into an ongoing project at BFH. We also thank Martin Wiederkehr, Urs Uehlinger, and Jérôme Voisard for their assistance and contribution to this study. We received further support and advice from Prof. Dr. Steffen Franke, for which we thank him. We thank Bernhard Bieri from Wenger Fenster AG for providing us with further background information.

References

- [1] S. Lindvall, Comparison of centralized and decentralized ventilation in a multifamily building in Stockholm. KTH Royal Institute of Technology, Stockholm, 2018.
- [2] S. M. F. S. D. W. Alexander Merzkirch, Field tests of centralized and decentralized ventilation units in residential buildings – Specific fan power, heat recovery efficiency, shortcuts and volume flow unbalances. *Energy and Buildings*, vol. 116, pp. 376-383, 2016.
- [3] M. K. K. H. L. Luca Baldini, Decentralized cooling and dehumidification with a 3 stage LowEx heat exchanger for free reheating Energy Build. *Energy and Buildings*, vol. 76, no. June 2014, pp. 270-277, 2014.
- [4] L. B. Moon Keun Kim, Energy analysis of a decentralized ventilation system compared with centralized ventilation systems in European climates: Based on review of analyses. *Energy and Buildings*, vol. 111, no. 1 January 2016, pp. 424-433, 2016.
- [5] S. P. T. K. Jinuk Lee, Development of a Ventilation System Using Window Cavity. *Sustainability*, no. 12 October 2020, 2020.
- [6] A. M. Shiva Najaf Khosravi, A CFD-Based Parametric Thermal Performance Analysis of Supply Air Ventilated Windows. *Energies*, no. 23 April 2021, 2021.
- [7] SIA 382 - 5: Mechanische Lüftung in Wohngebäuden, Schweizerischer Ingenieur- und Architektenverein.
- [8] F. R. Menter, Two-Equation Eddy-Viscosity Turbulence Models for Engineering Applications. *AIAA Journal*, vol. 32, no. 8. August 1994, pp. 1598-1605, 1994.